

# Maximum Power Extraction from an Optimal PV Array Configuration under various Partial Shading Conditions using MPPT

V Madhusudhan\*<sup>1</sup>, D Kiran Kumar<sup>2</sup>

<sup>1</sup>M.Tech, Power Electronics, JNTUH, Hyderabad, India

<sup>2</sup>Asst. Professor, Electrical and Electronics Engineering, JNTUH, Hyderabad, India

## Correspondence

\*V Madhusudhan

Electrical and Electronics Engineering Department,

JNTUH, Hyderabad, India

Email: madhuvishwa96@gmail.com

## Abstract:

*Photovoltaic power generation is considered the most reliable renewable energy option because of its plentiful availability, environmental friendliness, and minimal maintenance requirements. Partial Shading Conditions induce Mismatching Power losses, due to the formation of hotspots which causes output power reduction from Photovoltaic (PV) arrays. On performance curves i.e., power-voltage(P-V) and current-voltage (I-V), the partial shading also displays several maximum power points (MPP) and non-linearity, making it challenging to track the global maximum power point (GMPP). When PV modules are placed in an array under partial shading conditions, looking at the optimal configuration of the modules during the study enables us to extract the maximum power possible while minimizing the number of power peaks. In this paper, performance of the triple-tied (TT) configuration is compared with total-cross-tied (TCT) solar PV array configuration under various partial shading conditions by considering 7\*7 PV array. Four different shading scenarios are considered while evaluating performance of the PV array configurations. The performance analysis is done using the factors such as, efficiency, open circuit voltage, short circuit current, fill factors, voltage and currents at GMPPs and mismatching power losses. Maximum power is extracted from the triple-tied (TT) configuration under various shading conditions for the Standalone PV applications, using the Perturb and Observe algorithm in MPPT controller using the boost converter. The whole system is modelled and simulated in Matlab/Simulink using KC-200GT PV Module.*

## Keywords:

Maximum Power point Tracking, PV Array Configurations, Partial Shading Conditions, Triple-Tied PV Configuration.

## I. INTRODUCTION

Environmental problems have to be given more consideration because fossil fuels are widely used to generate electricity. The best options for addressing the challenges caused by the use of fossil fuels and fulfilling the world's rising energy needs are renewable energy sources [1]. The most promising renewable energy source is photo voltaic (PV) power generation because of its many benefits, including pollution-free operation, low maintenance requirements, increased abundance, and government support in the form of enticing incentives and subsidies for customers. However, the PV modules are expensive to install and have a poor energy conversion efficiency. Temperature (T) and the incidence of solar insolation (G) determine the PV system's output primarily [2]. PV modules experience uniform insolation levels with uniform insolation, which results in only one maximum power point (MPP) on the P-V curve that is convenient to measure using standard maximum power point tracking (MPPT) algorithms [3]. The operation of the PV system gets significantly impacted

by partial shadowing conditions (PSCs), which can be caused on by snow cover, chimneys, trees, passing clouds, bird droppings, and other variables [4]. PV modules under PSCs experience varying degrees of insolation, which leads to mismatched power losses and the development of hot spots in shaded PV modules. An antiparallel diode known as a bypass diode can be connected across the PV module to prevent hot spot issues [5]. Nevertheless, there will be several MPPs in the P-V curve because of the bypass diode's connection. Among these MPPs, the others are known as the local maximum power points (LMPPs), while one is known as the global maximum power point (GMPP). PSCs cause the PV system's power production to decrease and mismatching power losses to rise. Several researchers have proposed a range of approaches in the literature to address these PSC issues, including MPPT tracking strategies, converter-based architectures integrated with the PV system, and PV array fixed-configuration and reconfiguration methodologies. To precisely track the GMPP under PSCs, diverse MPPT approaches are proposed in the literature [6]-[9].

Configurations of PV arrays are a technique to reduce mismatching power losses and increase efficiency SP, TCT, and BL PV array topologies under various shading circumstances were studied by Smita Pareeka *et al.* [10]. A detailed evaluation of five PV configurations, including S, SP, TCT, BL, and HC, was conducted by Bingol O *et al.* [11] using a 6x 6 PV array which was simulated in the MATLAB/Simulink environment. A distributed maximum power point approach (D-MPPT) was proposed at the module level by Marco Balato *et al.* [12]. This system uses a separate MPPT controller at each PV module and equips each module with a micro inverter. This method's disadvantage is that it requires a large number of micro inverters and sensors, and it is expensive to implement. From the gaps found in the earlier research, to reduce the issues pertaining to PSC's the comparison of performance of TT and TCT configurations is done and maximum power is extracted using P&O MPPT algorithm for the standalone PV applications.

## II. MODELLING OF THE PV ARRAY

The basic power conversion component of a photovoltaic power generation system is a PV module. The incidence of solar insolation (G) and temperature (T) have the largest influences on the electrical output of the PV module. A single diode model is more frequently employed since solving the non-linear equations of two diode models requires significant effort and computational speed is low [13],[14].

Fig.1(a) depicts the practical equivalent circuit for a single-diode PV module model and it has a current source in parallel with a diode. PV array modeling and simulation in MATLAB/Simulink is done using the KYOCERA-KC200GT PV module and the parameters are given in Table. I .

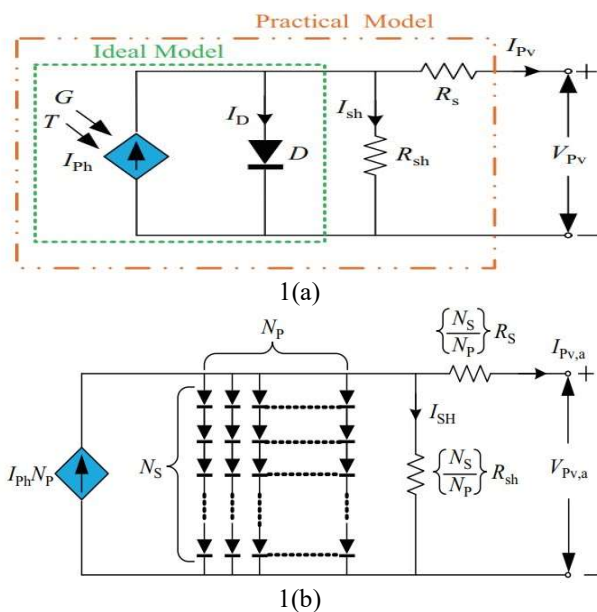


Fig.1 (a) PV module equivalent Circuit (b) PV Array equivalent circuit.

The mathematical relation between the current and voltage of the PV module is illustrated by Eq. (1).

$$I_{Pv} = I_{Ph} - I_r \left[ \exp \left( \frac{q(V_{Pv} + R_s I_{Pv})}{n_s k T a} \right) - 1 \right] - \frac{V_{Pv} + R_s I_{Pv}}{R_{sh}} \quad (1)$$

where  $I_{pv}$  is the generated photon current due to solar irradiance in a module (A),  $I_r$  is the diode's reverse saturation current [A],  $V_{Pv}$  is the PV module voltage [V],  $V_T$  is the thermal voltage of the PV cell,  $T$  is the temperature at which the PV module is operated [K],  $K$  is the constant of Boltzmann,  $q$  is the electron charge,  $R_s$  and  $R_{sh}$  are the series and shunt resistances in [ $\Omega$ ], ' $a$ ' is the ideality factor of the diode.

The PV array is created by interconnecting the necessary number of PV modules in series or parallel to produce the required voltage and current. Fig.1(b) depicts the equivalent circuit for a PV array.

The mathematical relation between the current and voltage of the PV array is illustrated by Eq. (2) [15].

$$I_{Pv,a} = I_{Ph} N_p - I_r N_p \left[ \exp \left( \frac{q(V_{Pv,a} + R_s \left( \frac{N_s}{N_p} \right) I_{Pv,a})}{n_s k T a} \right) - 1 \right] - \frac{V_{Pv,a} + R_s \left( \frac{N_s}{N_p} \right) I_{Pv,a}}{R_{sh} \left( \frac{N_s}{N_p} \right)} \quad (2)$$

where  $N_s$  is the number of PV modules connected in series,  $N_p$  is the number of PV modules connected in parallel,  $I_{Pv,a}$  and  $V_{Pv,a}$  are the output current and output voltage of the PV array. It is evident from Fig. 2(b) that the maximum power output of the PV module decreases as the irradiance levels drops.

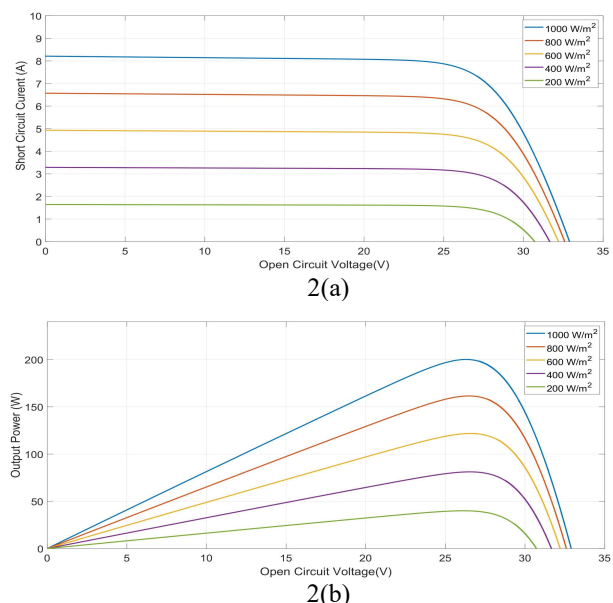


Fig.2 (a) I-V Characteristics and (b) P-V Characteristics of the PV module under various Solar Irradiance levels and constant temperature

### III. VARIOUS SHADING PATTERNS

This section describes the different types of shading scenarios considered under Partial shading conditions. To analyze the performance of  $7 \times 7$  PV array Configurations, various shading scenarios are considered depending upon the solar irradiance level on the PV module, the shading scenarios are categorized into corner, center, diagonal and right side end shadings as shown in Fig. 3. The number of rows, columns, as well as the PV module's solar irradiance levels are indicated by the X, Y, and Z axes, respectively in Fig. 4. The solar insolation level on each PV module and all shading conditions are interpreted as follows:

#### A. Corner Shading scenario

In this shading situation, the PV modules on the left side corner of the  $7 \times 7$  PV array are shaded with varying levels of solar insolation, and the rest of the PV modules insolated at  $1000 \text{ W/m}^2$  respectively as shown in Fig. 3(a).

#### B. Center Shading scenario

In this shading situation, the PV modules in the center of the  $7 \times 7$  PV array are shaded with varying levels of solar insolation, and the remaining of the PV modules insolated at  $1000 \text{ W/m}^2$  respectively as shown in Fig. 3(b).

#### C. Diagonal Shading scenario

In this shading situation, if diagonal modules of an  $7 \times 7$  array are unevenly shaded, with varying levels of solar insolation, then, it is called diagonal shading, and the remaining of the PV modules insolated at  $1000 \text{ W/m}^2$  respectively, which is represented in Fig. 3(c).

#### D. Right-Side end shading scenario

In this shading situation, the PV modules located on the right-side end of the  $7 \times 7$  PV array are unevenly shaded with different levels of solar insolation, are referred to as right-side end shading and the rest of the PV modules insolated at  $1000 \text{ W/m}^2$  respectively as shown in Fig. 3(d).

TABLE I.  
PV MODULE SPECIFICATIONS

S.No.	Parameter	Value
1	Peak Power, $P_m$	200.143W
2	Peak Power Current, $I_{mp}$	7.61 A
3	Peak Power Voltage, $V_{mp}$	26.3 V
4	Open Circuit Voltage, $V_{OC}$	32.9 V
5	Short Circuit Current, $I_{SC}$	8.21 A
6	Temperature co-efficient of $V_{OC}$ , $K_V$	-0.123V/K
7	Temperature co-efficient of $I_{SC}$ , $K_I$	0.0032A/K
8	Ideality factor of a Diode, $a$	1.3
9	Number of series connected cells in a module, $n_s$	54
10	PV module dimensions (Area)	1425 mm $\times$ 990 mm

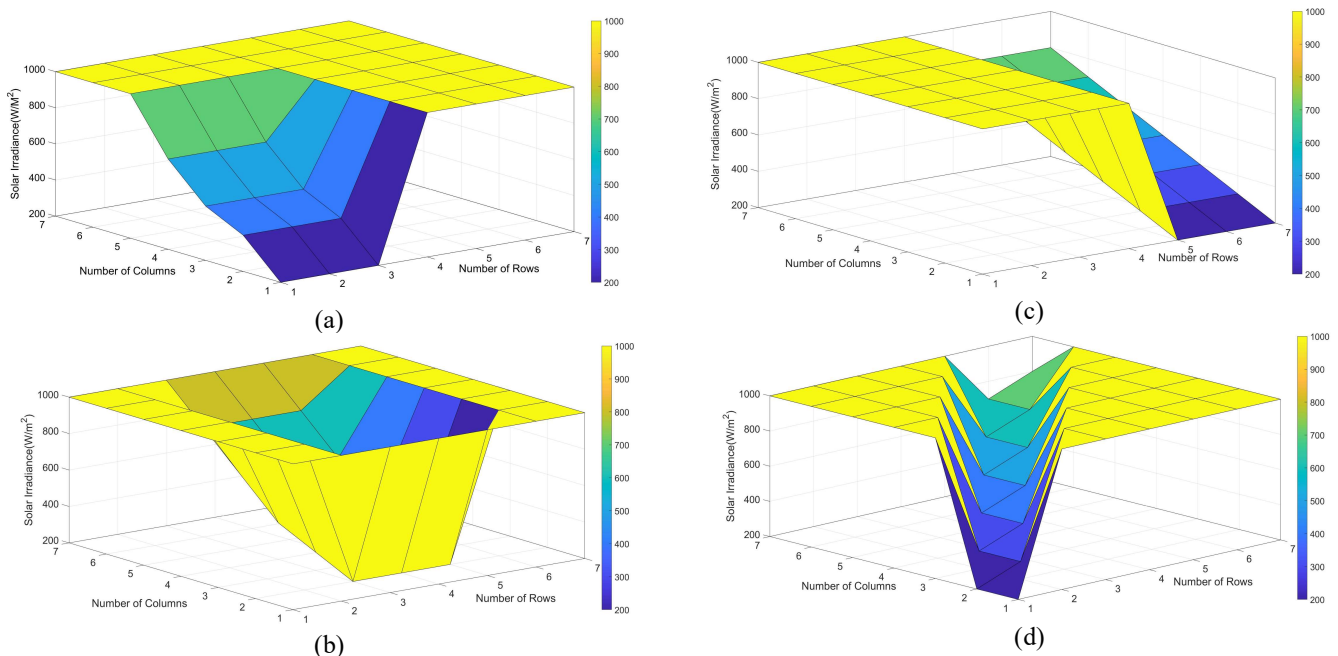


Fig. 3. Various Partial Shading Scenarios: (a) Corner (b) Center (c) Diagonal and (d) Right side end Shading.

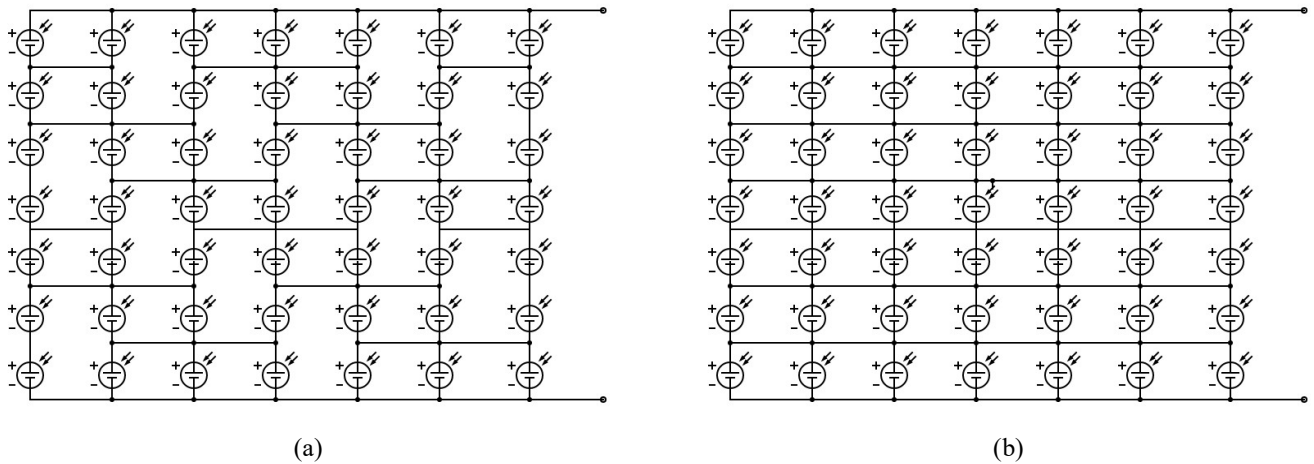


Fig. 4. An Illustrative diagram of 7×7 PV Array configurations. (a) Triple-Tied configuration. (b) Total-Cross-Tied configuration.

**IV. MODELLING OF PV ARRAY CONFIGURATIONS**

The modeling and simulation of various 7×7 solar PV configurations under various PSC's are explained in this section. The Matlab/Simulink program is used to implement all PV configurations. This section additionally discusses the simulation findings, namely the I-V and P-V characteristics of PV configurations under the uniform and four shading situations. PV array setup simulations are run at a constant temperature of 25 °C and various insolation levels. Assume that  $I_K$  and  $I_{Sr}$  are the module current and string current, respectively, and that  $V_K$  is the module voltage,  $V_{RW}$  is the row voltage.

*A. Triple-Tied (TT)*

The TT arrangement, which modifies the Bridge-Link layout, takes its cues from the stairwell's flights [16],[17]. In this arrangement Fig. 4(a), three modules are connected in a row after which there is a space. The first two strings in this row are cross-tied, followed by a gap, the third through fifth strings are cross-tied, followed by a gap, and the sixth and seventh strings are cross-tied. Similar to the first row, the second row's first three strings are cross-tied, followed by a gap strings 4th to 6th are cross-tied, and the third row's second to fourth strings are cross-tied, followed by a gap, and the third row's fifth to seventh strings are cross-tied. Repeating this pattern makes up the remaining rows. Fig.5(a,b) demonstrates the simulation outcomes for the TT PV arrangement for various PSCs. The output current ( $I_{Pv}$ ), output voltage ( $V_{Pv}$ ) and the output power ( $P_{Pv}$ ) of the TT PV array configuration is calculated by eq. 3.eq. 4 and eq. 5.

$$I_{Pv} = I_1 + I_8 + I_{15} + I_{22} + I_{29} + I_{36} + I_{43} = 7 \times I_K \quad (3)$$

$$V_{Pv} = V_1 + V_2 + \dots + V_7 = \sum_{K=1}^7 V_K = 7 V_K \quad (4)$$

$$P_{Pv} = V_{Pv} \times I_{Pv} \quad (5)$$

*B. Total-Cross-Tied(T-C-T)*

To counteract the effects of partial shade in the SP PV arrangement, the TCT configuration is modeled [16], [18]. The cross-tied formation is another name for this arrangement. Shaded modules under PSCs are given an alternate route since there are cross-ties between the modules. By doing this, hotspot issues and the necessity for bypass diodes are avoided. Many PV modules are equipped with by-pass diodes to mitigate the effects of shading. However, if these diodes are faulty or insufficient, hotspots may still occur. The TCT configuration is modelled as follows: each row is first placed in series with the rows after it, with all the PV modules in strings originally arranged parallel as rows as shown in Fig.4(b). By-pass diodes allow the current to bypass the shaded cells, preventing them from becoming reverse biased. The output voltage of the PV array is the total of the individual row voltages in this design, where the voltage across each row is equal to the voltage across each module. The output current of the PV array is the total of the individual module currents in a row in this design. Fig.5(c,d) demonstrates the simulation outcomes for the T-C-T PV arrangement for various PSCs. The output current ( $I_{Pv}$ ), output voltage ( $V_{Pv}$ ) and the output power ( $P_{Pv}$ ) of the T-C-T PV array configuration is calculated by below equations.

$$I_{Pv} = I_1 + I_8 + I_{15} + I_{22} + I_{29} + I_{36} + I_{43} = 7 \times I_K \quad (6)$$

$$V_{RW1} = V_{RW2} = V_{RW3} = \dots = V_{RW7} = V_K \quad (7)$$

$$V_{Pv} = V_{RW1} + V_{RW2} + V_{RW3} + V_{RW4} + V_{RW5} + V_{RW6} + V_{RW7} \quad (8)$$

$$P_{Pv} = V_{Pv} \times I_{Pv} \quad (9)$$

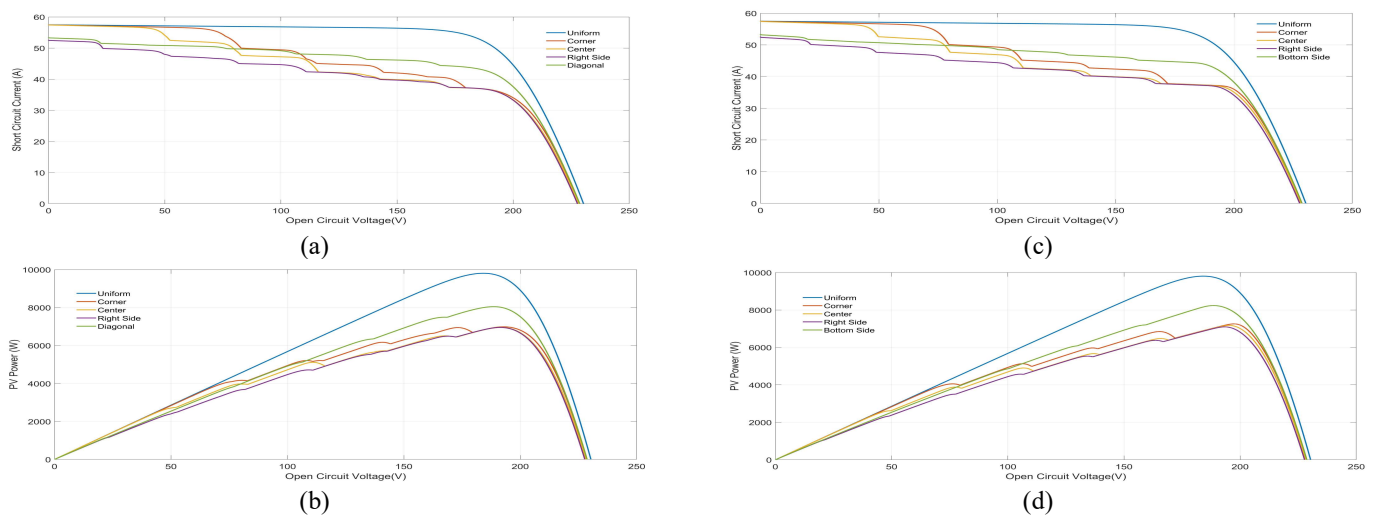


Fig.5 I-V and P-V Curves of PV Array Configurations under various PSC's: (a,b) Triple-Tied and (c,d) Total-Cross-Tied Configurations.

## V. ANALYSIS OF PERFORMANCE FACTORS

Analysis of the PV configuration's functionality is done by taking into account certain factors such as, efficiency, fill factors, and mismatching power losses. By evaluating these parameters, we will be able to determine which PV configuration will provide the highest performance when compared to other options.

### Mismatching Power Loss:

The ratio of the variation in peak power from uniform irradiance to partial shading scenarios divided by the peak power produced under uniform insolation is known as the mismatching power loss [16]. The mismatching power loss is computed by Eq. 5. and it is expressed in percentage.

$$\Delta P_{MPL}(\%) = \frac{P_{MPP,UIC} - P_{MPP,PSC}}{P_{MPP,UIC}} \times 100 \quad (10)$$

where,  $\Delta P_{MPL}$  is the mismatching power loss,  $P_{MPP,UIC}$  is the maximum power produced under uniform irradiance and  $P_{MPP,PSC}$  is the maximum power produced under PSC.

### Fill Factor:

It is defined as the ratio between global peak power to the product of open circuit voltage and short circuit current. For a PV module, maximum current and voltage are the short circuit current ( $I_{sc}$ ) and open circuit voltage ( $V_{oc}$ ). Practically, the power generated from the PV module is zero at these operating points. Maximum power from a solar cell can be determined by using Fill Factor (FF),

$$Fill\ Factor\ (FF) = \frac{V_m \times I_m}{V_{oc} \times I_{sc}} \quad (11)$$

### Efficiency:

The most used criterion for comparing PV module performance is efficiency. The spectrum, intensity of the

incident sunlight, and temperature of the PV module all affect a PV module's efficiency. Efficiency ( $\eta$ ) is the ratio of the maximum power produced to the solar power input to the panels.

$$Efficiency(\eta) = \frac{V_{mpp} \times I_{mpp}}{L \times A} \quad (12)$$

where ' $\eta$ ' is the efficiency,  $V_{MPP}$  and  $I_{MPP}$  are the voltage and currents at peak power points, ' $L$ ' is the solar intensity fall on the PV panel per ' $m^2$ ' and ' $A$ ' is the area of the PV panel.

### 1) Analysis Under Uniform Irradiance:

Every PV module is exposed to a constant insolation of  $1,000\text{ W/m}^2$  under the uniform insolation condition. According to the simulation results, both PV configurations under consideration produce a single GMPP in the P-V curve and the same amount of peak power.  $9,807.00\text{ W}$  is the total power generated. For both setups, the mismatching power losses are zero. Table I(a) provides the performance parameter values. For both PV arrangements, FF has the same value of 74%.

### 2) Analysis Under Corner Shading:

Performance specifications of T-T and T-C-T configurations corner shading can be observed in Table.2, respectively. It is observed that the T-C-T configuration has improved performance in GMPP by 3.75% compared to T-T configuration. Both the configurations produce four LMPP's. The power enhancement of the TCT PV configuration over TT PV configuration is  $272.15\text{ W}$

### 3) Analysis Under Center Shading:

Performance specifications of T-T and T-C-T configurations center shading can be observed in Table.2, respectively. According to the simulation results, T-T and T-C-T PV configurations under consideration produce peak power of  $6952.18\text{ W}$  and  $7173.09\text{ W}$  respectively.

#### 4) Analysis Under Diagonal Shading:

The highest global peak power of 8,236.6 at 188.5500 V and 43.6837 A without LMPPs is produced by the TCT PV system under this shading scenario. Performance specifications of T-T and T-C-T configurations diagonal shading can be observed in Table.2, respectively. The power improvement of TCT PV configuration over TT PV configuration is 189.5 W

#### 5) Analysis Under Right-side End Shading:

With four LMPPs, the TCT PV configuration provides the highest global peak output of 7,097.70 W at 193.3200 V and 36.7148 A under this shading condition. Performance specifications of T-T and T-C-T configurations diagonal shading can be observed in Table.2, respectively. The mismatching power loss is lower for TCT compared to the TT configuration

**TABLE. 2**  
**PERFORMANCE PARAMETERS UNDER VARIOUS PARTIAL SHADING CONDITIONS**

<b>a. Triple-Tied Configuration</b>								
Shading Pattern	V <sub>oc</sub> (V)	I <sub>sc</sub> (A)	V <sub>MPP</sub> (V)	I <sub>MPP</sub> (A)	P <sub>MPP</sub> (A)	ΔP <sub>MPL</sub> (%)	FF(%)	η(%)
Uniform	230.28	57.60	184.10	53.27	9806.64	0.00	73.94	14.19
Centre	228.15	57.57	191.72	36.26	6952.18	29.11	52.93	12.05
Corner	228.60	57.58	192.82	36.22	6984.89	28.77	53.06	11.68
Diagonal	228.65	53.44	188.53	42.68	8046.63	17.95	65.85	13.52
Right side end	227.68	52.62	191.35	36.33	6951.05	29.12	58.02	12.80

<b>b. Total-Cross-Tied Configuration</b>								
Shading Pattern	V <sub>oc</sub> (V)	I <sub>sc</sub> (A)	V <sub>MPP</sub> (V)	I <sub>MPP</sub> (A)	P <sub>MPP</sub> (A)	ΔP <sub>MPL</sub> (%)	FF(%)	η(%)
Uniform	230.28	57.60	184.10	53.27	9806.64	0.00	73.94	14.19
Centre	228.25	57.57	195.25	36.74	7173.09	26.85	54.59	12.43
Corner	228.63	57.58	197.35	36.77	7257.04	26.00	55.13	12.13
Diagonal	228.68	53.41	188.53	43.69	8236.04	16.02	67.43	13.83
Right side end	227.70	52.59	193.32	36.71	7097.26	27.63	59.27	13.07

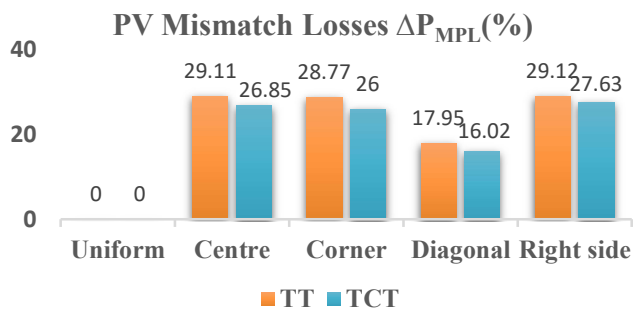


Figure 6

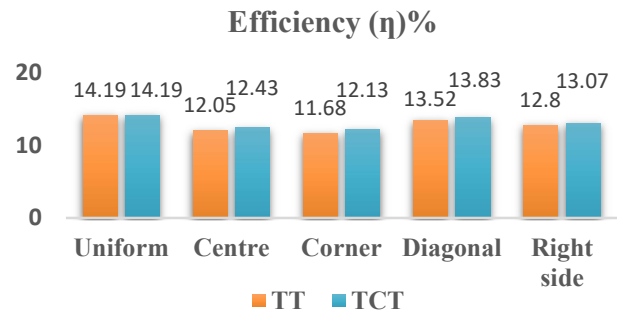


Figure 7

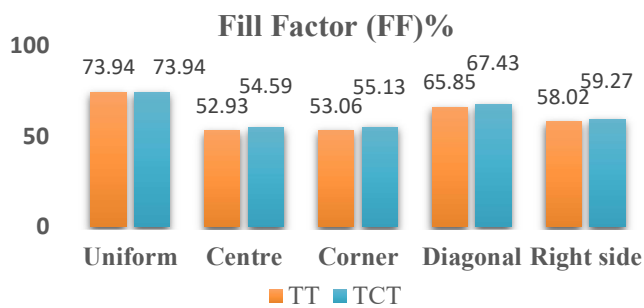


Figure 8

**TABLE. 3**  
**REDUCED NUMBER OF CROSS TIES IN T-T COMPARED TO T-C-T**

S.No.	Array Size	Reduced Number of Cross-Ties
1	6*6	8
2	7*7	12
3	8*8	16
4	9*9	20

### VI. MAXIMUM POWER EXTRACTION

The Perturb and Observe (P&O) algorithm in MPPT is implemented for the extraction of maximum power under various partial shading conditions for the Triple-Tied and Total-Cross-Tied configurations, by considering DC Load (Resistive) for the PV Standalone applications.

The approach was to achieve maximum power extraction for 7\*7 PV array under different shading scenarios by continuously adjusting the operating point across the maximum power point using the P&O algorithm which provides feedback to the Boost Converter, which is fed by the PV system’s output. The boost converter parameters and their values are represented in Table.3

In the Triple-Tied Configuration output power for the Uniform, Centre, Corner, Diagonal and Right-side end shading scenarios is 9806.64 W, 6952.18 W, 6984.89 W, 8046.63 W and 6951.05 W respectively. Similarly, in the Total-Cross-Tied Configuration output powers for the Uniform, Centre, Corner, Diagonal and Right-side end shading scenarios is 9806.64 W, 7173.09 W, 7257.04 W, 8236.04 W and 7097.26 W respectively.

In order to extract the power equivalent to the PV output power, boost converter is designed to maintain the PV output voltage ( $V_{PV}$ ) around maximum voltage ( $V_{MPP}$ ) point, which is obtained at maximum power ( $P_{MPP}$ ).

TABLE. 4

	Boost Converter Components	Parameter Value
1	Input Capacitance	5mF
2	Inductance	0.05 H
3	Switching frequency	5 kHz
4	Output Capacitance	5mF
5	Load Resistance	13.5 $\Omega$

### VI. RESULTS AND DISCUSSION

TT and TCT PV configurations under the uniform isolation condition and four distinct shading scenarios are simulated using the MATLAB/Simulink platform.

Comparisons of the PV output power and Load output power for TT configuration under Uniform, Centre, Corner, Diagonal and Right-side end shading scenarios are shown in Fig.9, Fig.10, Fig.11, Fig.12, and Fig.13 respectively. In TT configuration Output power across load extracted for the Uniform, Centre, Corner, Diagonal and Right-side end shading scenarios is 9462 W, 6612 W, 6894 W, 8007 W and 6603 W respectively.

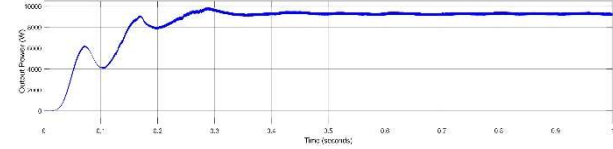
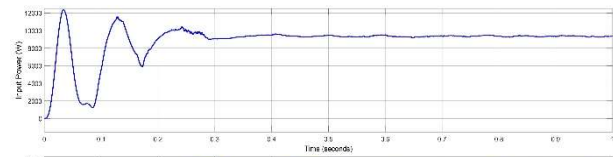


Fig. 9. PV power and Load Power in Uniform Insolation

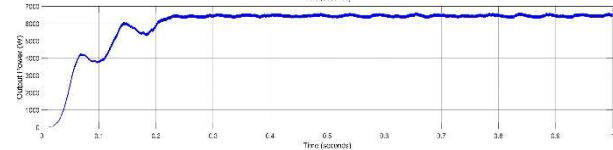
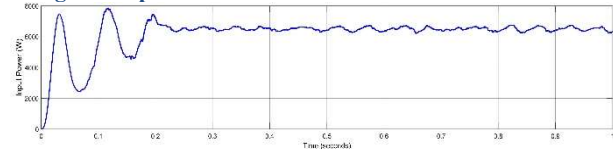


Fig. 10. PV power and Load Power in centre shading

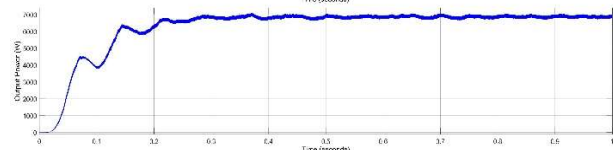
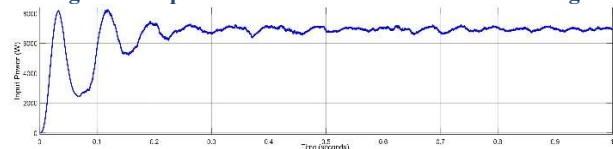


Fig. 11 PV power and Load Power in corner shading

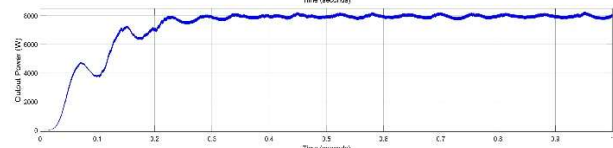
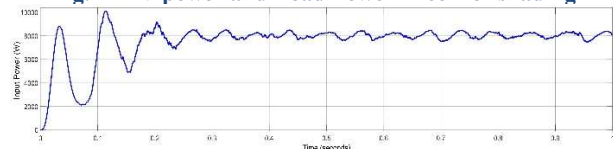


Fig. 12 PV power and Load Power in Diagonal shading

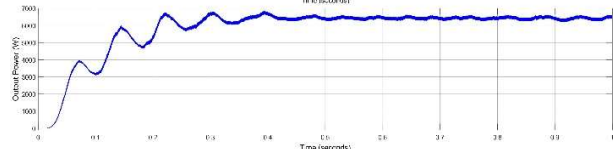
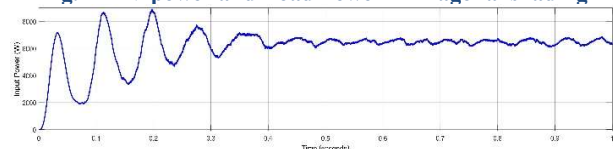


Fig. 13. PV power and Load Power in Rightside end shading

## REFERENCES:

- [1] A. Strzalka, N. Alam, E. Duminil, V. Coors, and U. Eicker, "Large scale integration of photovoltaics in cities", *Applied Energy*, vol. 93, pp. 413–421, May 2012.
- [2] P. Manganiello, M. Balato, and M. Vitelli, "A survey on mismatching and aging of PV modules: the closed loop," *IEEE Transactions on Industrial Electronics*, vol. 62, no. 11, pp. 7276–7286, Nov. 2015.
- [3] B. Subudhi and R. Pradhan, "A comparative study on maximum power point tracking techniques for photovoltaic power systems," *IEEE Transactions on Sustainable Energy*, vol. 4, no. 1, pp. 89–98, Jan. 2013.
- [4] A. S. Rana, M. Nasir, and H. A. Khan, "String level optimization on grid-tied solar PV systems to reduce partial shading loss," *IET Renewable Power Generation*, vol. 12, no. 2, pp. 143–148, Feb. 2018.
- [5] S. W. Ko, Y. C. Ju, H. M. Hwang, J. H. So, Y. S. Jung, H. J. Song, H. E. Song, S. H. Kim, and G. H. Kang, "Electric and thermal characteristics of photovoltaic modules under partial shading and with a damaged bypass diode," *Energy*, vol. 128, pp. 232–243, Jun. 2017.
- [6] J. P. Ram, T. S. Babu, and N. Rajasekar, "A comprehensive review on solar PV maximum power point tracking techniques," *Renewable and Sustainable Energy Reviews*, vol. 67, pp. 826–847, Jan. 2017.
- [7] A. R. Jordehi, "Maximum power point tracking in photovoltaic (PV) systems: a review of different approaches," *Renewable and Sustainable Energy Reviews*, vol. 65, pp. 1127–1138, Nov. 2016.
- [8] M. A. M. Ramli, S. Twaha, K. Ishaque, and Y. A. Al-Turki, "A review on maximum power point tracking for photovoltaic systems with and without shading conditions," *Renewable and Sustainable Energy Reviews*, vol. 67, pp. 144–159, Jan. 2017.
- [9] K. Ishaque and Z. Salam, "A review of maximum power point tracking techniques of PV system for uniform insolation and partial shading condition," *Renewable and Sustainable Energy Reviews*, vol. 19, pp. 475–488, Mar. 2013.
- [10] S. Pareek and R. Dahiya, "Output power maximization of partially shaded 4\*4 PV field by altering its topology," *Energy Procedia*, vol. 54, pp. 116–126, 2014.
- [11] O. Bingol and B. " Ozkaya, "Analysis and comparison of different PV " array configurations under partial shading conditions," *Solar Energy*, vol. 160, pp. 336–343, Jan. 2018.
- [12] M. Balato, L. Costanzo, and M. Vitelli, "DMPPT PV system: modeling and control techniques," *Advances in Renewable Energies and Power Technologies*, I. Yahyaoui, Ed. Amsterdam: Elsevier, 2018, pp. 163–205.
- [13] M. Suthar, G. K. Singh, and R. P. Saini, "Comparison of mathematical models of Photo-Voltaic (PV) module and effect of various parameters on its performance," in *Proceedings of 2013 International Conference on Energy Efficient Technologies for Sustainability*, 2013, pp. 1354–1359.
- [14] M. A. Hasan and S. K. Parida, "An overview of solar photovoltaic panel modeling based on analytical and experimental viewpoint," *Renewable and Sustainable Energy Reviews*, vol. 60, pp. 75–83, Jul. 2016.
- [15] M. G. Villalva, J. R. Gazoli, and E. R. Filho, "Comprehensive approach to modeling and simulation of photovoltaic arrays," *IEEE Transactions on Power Electronics*, vol. 24, no. 5, pp. 1198–1208, May 2009.
- [16] S. R. Pendem, S. Mikkili, and P. K. Bonthagorla, "PV distributed-MPP tracking: total-cross-tied configuration of string-integrated-converters to extract the maximum power under various PSCs," *IEEE Systems Journal*, vol. 14, no. 1, pp. 1046–1057, Mar. 2020.
- [17] G. Cipriani, V. Di Dio, D. La Manna, R. Miceli, and G. R. Galluzzo, "Technical and economical comparison between different topologies of PV plant under mismatch effect," in *Proceedings of the 2014 Ninth International Conference on Ecological Vehicles and Renewable Energies*, 2014, pp. 1–6.
- [18] C. T. K. Kho, J. Ahmed, Y. L. Then, and M. Kermadi, "Mitigating the effect of partial shading by triple-tied configuration of PV modules," in *Proceedings of 2018 IEEE PES Asia-Pacific Power and Energy Engineering Conference*, 2018, pp. 532–537.